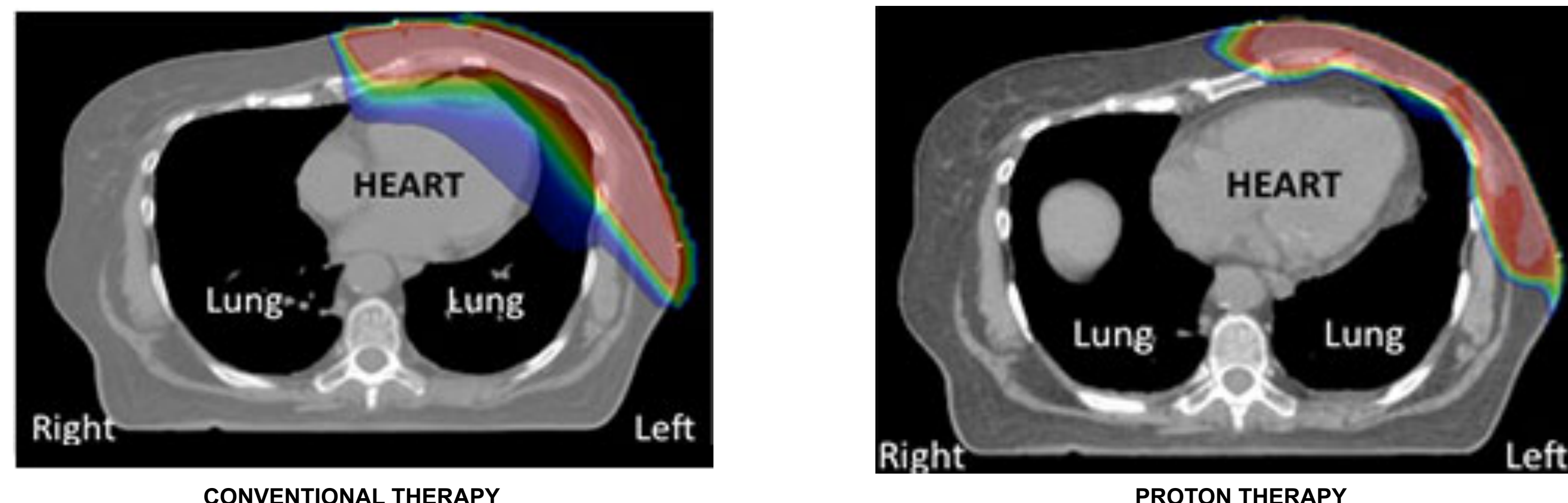


## I. INTRODUCTION

- Over 40,000 women will die from breast cancer (BC) in the United States in 2017.<sup>1</sup>
- Radiotherapy (RT) is a critical component of breast cancer management, yielding a substantial survival benefit<sup>2</sup> but can result in inadvertent exposure of large volumes of normal tissues to low and moderate doses of radiation.
- There is a 7% increase in relative risk (RR) of cardiac disease with each 1-Gy increase in mean heart dose, or 35% total for the typical patient.<sup>3</sup>
- Left-sided BC patients who receive RT to the chest wall have a 4-fold higher risk of cardiac events than patients with right-sided BC.<sup>4</sup>
- Because cardiac injury is known risk of treatment, early markers of heart injury could be beneficial for follow-up management in these patients and may help identify new techniques that would improve the therapeutic ratio of treatment.



**Figure 1: Treatment Planning for Photon vs Proton Therapy:** These figures represent radiation treatment planning on chest CT scans for left sided breast cancer patients. The colors represent the amount of radiation exposure. The figure on the left shows radiation treatment planning for conventional X-ray therapy and the figure on the right shows the plan for the same patient but for proton therapy treatment.

**OBJECTIVE :** To correlate regional RT dose with regional myocardial strains from cardiac magnetic resonance (CMR) images to quantify subclinical heart injury and compare risk of cardiac toxicity for standard X-ray based RT versus a proton therapy treatment in breast cancer patients.

## II. METHODOLOGY: IMAGING AND PREPROCESSING

### IMAGE ACQUISITION

- Images were acquired at 8-10 time points over the systolic phase of the cardiac cycle with parallel-tagging cardiac MR images, in patients with left-sided breast cancer under protocol UFPTI 1419- BR02. Images were acquired before and 6 to 12 months after completion of RT.

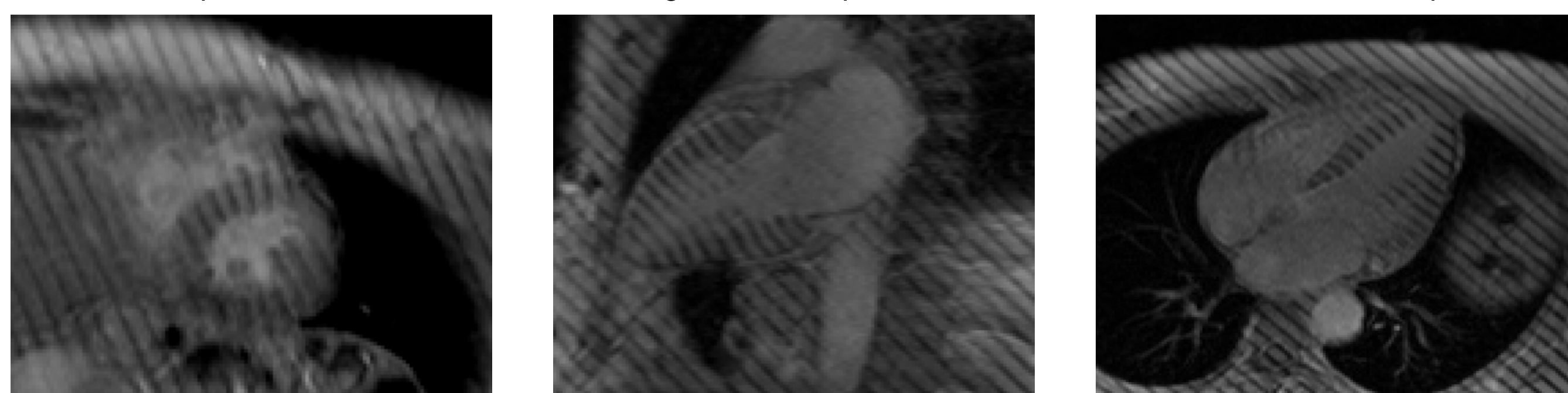


**Figure 2: Cardiac MR Images with Tags:** Representative short-axis and long-axis (2 and 4 chamber views) images are shown.

### HEART LEFT VENTRICLE CONTOUR SEGMENTATION

- An in-house semi-automatic snake based contouring toolkit was used to segment the Left Ventricle (LV) endocardial and epicardial borders on each image slice and time frame. Mathematical models for each surface (Fig. 3) were defined in a prolate spheroidal coordinate system (PSCS) (Eqn. 1) with  $\lambda$ , the radial coordinate, expressed as a series expansion in  $\theta$  and  $\mu$ , the circumferential and longitudinal angles.

$$\lambda(\mu, \theta) = \sum_{l=0}^L \sum_{m=-l}^l a_l P_l^{lm}(\cos \mu) \cdot \begin{cases} \sin m\theta & m > 0 \\ \cos m\theta & m \leq 0 \end{cases}$$

$$= a_0 + a_1 \sin(\mu) \sin(\theta) + a_2 \cos(\theta) + a_3 \sin(\mu) \cos(\theta) + a_4 \sin(\mu)^2 \cos(\theta)^2 + a_5 \cos(\mu) \sin(\mu) \cos(\theta) + a_6 (3 \cos(\mu)^2 - 1) + a_7 \cos(\mu) \sin(\mu) \sin(\theta) + a_4 \sin(\mu)^2 \sin(\theta)^2 + \dots$$

Eqn. 1

### DEFORMABLE IMAGE REGISTRATION

- The deformation of the heart LV was defined by modes of deformation in the local PSCS, followed by 3 rotations and 3 translations in x, y and z.
- These modes and motions were applied to de-warp the heart from the follow-up time frame back to the reference time when the tags were generated. Virtual tagged images were deformed according to the model and compared with the patient MR images to determine the modes.<sup>5,6</sup>

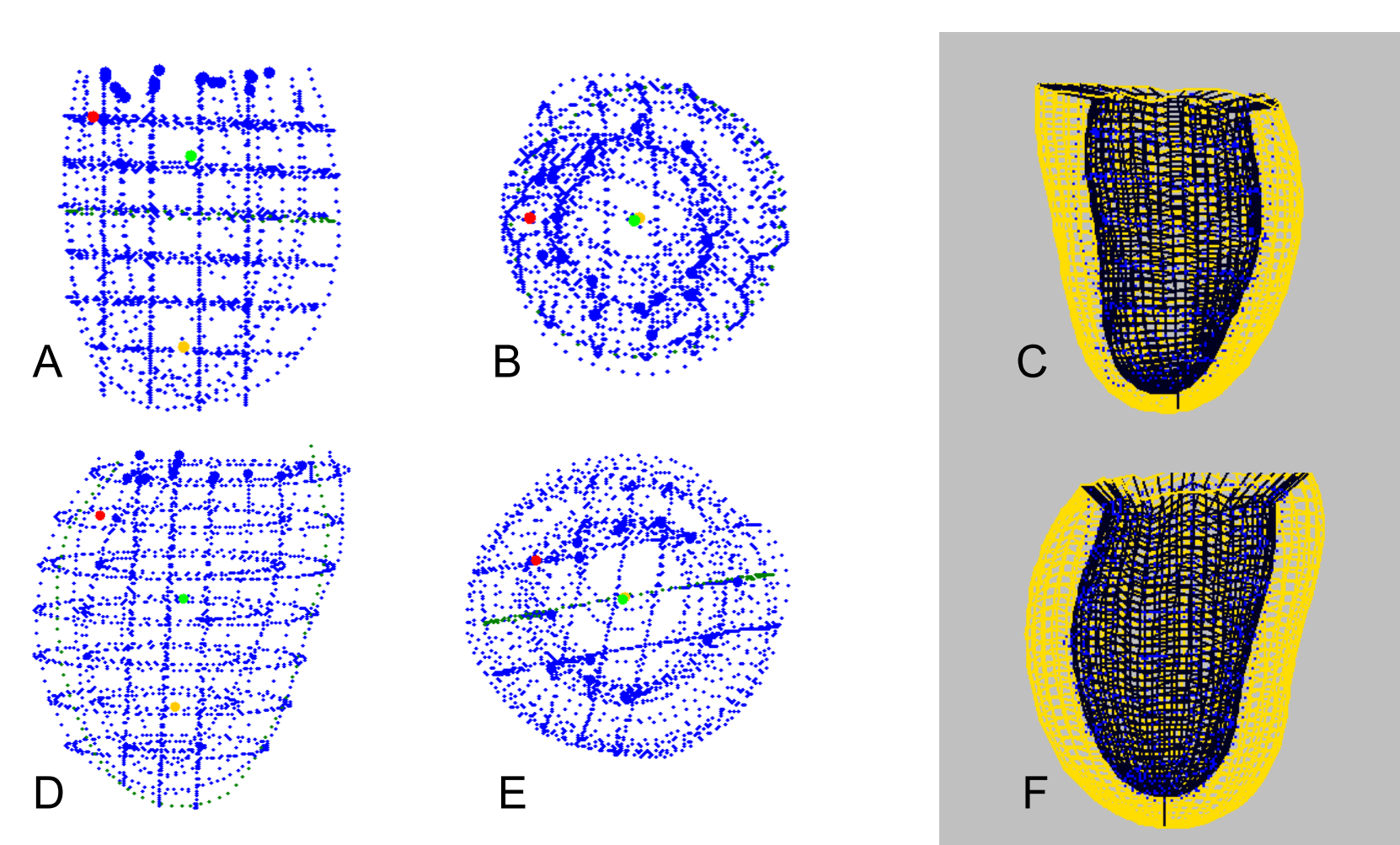


**Figure 3. Left ventricular epicardial and endocardial contour points and surface fits.** Pre-RT LV contour points are shown in the side [A] and top [B] views, along with the fitted 3D surface model [C]. The green, orange and red dots mark the centroid, apical focal point and mid-septum wall locations. [D]-[F] show the analogous data for the post-RT heart.

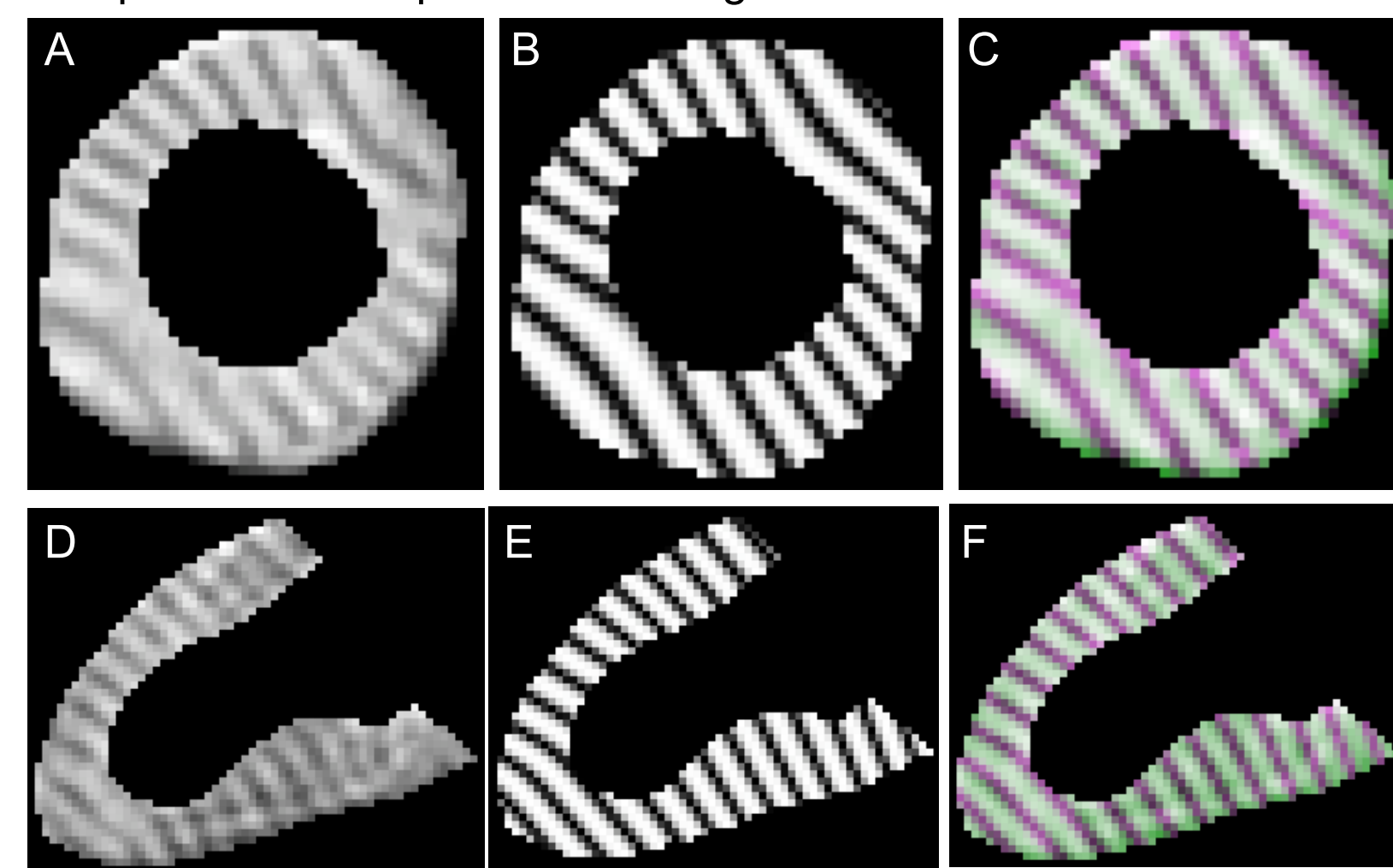


**Figure 4. Deformation modeling of parallel-tagged MR images.** [A] shows a tagged short-axis MR image at end-systole after applying a myocardial mask. [B] shows the deformed virtual tagged image at the same slice location and time. [C] shows a color overlay where dark green highlights the tags in the patient MR image, pink highlights tags in the virtual image, and darker pink results when they are well-aligned.

## ACKNOWLEDGEMENTS

Funding for this work is from the Ocala Royal Dames Foundation for Cancer Research, University Scholars Program and the UF Foundation.

## II. METHODOLOGY: STRAIN CALCULATIONS AND DOSE REGISTRATION

### STRAIN TENSOR COMPUTATION

- A 3D mesh of material points was generated with 5 layers radially, 6 longitudinally and 8 circumferentially. The 3D Lagrangian strain tensor,  $E$ , was calculated from the deformation gradient tensor,  $F$ , as  $E = \frac{1}{2}(F^T F - I)$ . Circumferential strain,  $E_{cc}$ , over the cardiac cycle is shown in Figure 5A.

### WALL THICKENING PARAMETER COMPUTATION

- An measure of fractional wall thickening<sup>6</sup>,  $T$ , at each material point was computed from the right stretch tensor,  $U$ , via Eqn. 2, where  $F = RU$ .

$$T = \frac{1.0 + U_{RC}(U_{CR}U_{LL}-U_{CL}U_{LR})-U_{RL}(U_{CR}U_{LC}-U_{CC}U_{LR})}{U_{CC}U_{LL}-U_{CL}U_{LC}} - 1.0$$

Eqn. 2

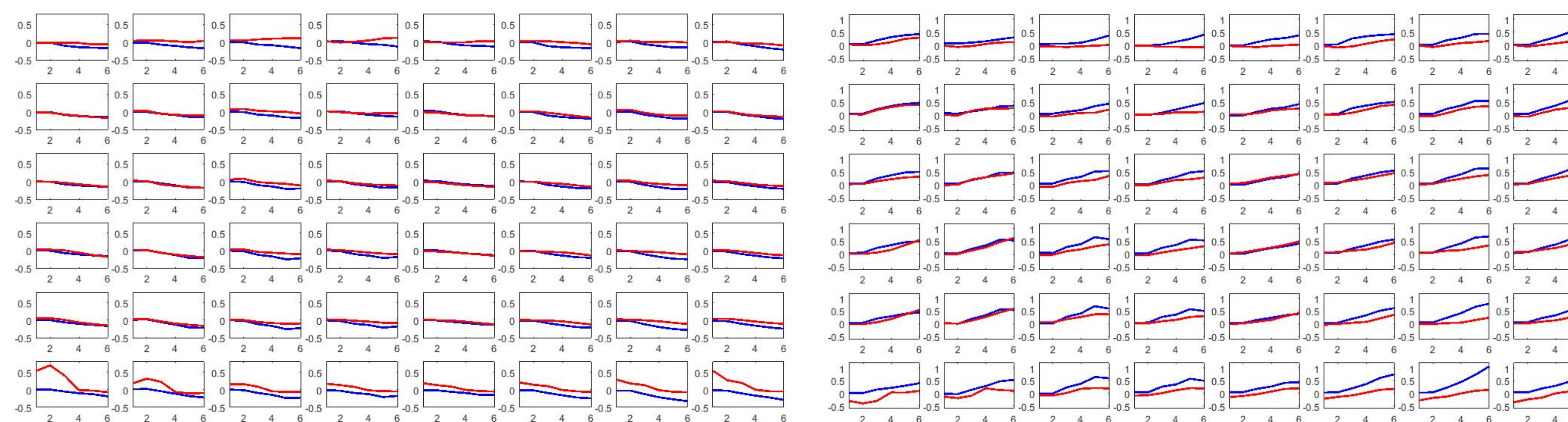


**Figure 5. Circumferential strains and wall thickness:** Each mini-plot shows strain on the vertical axis as a function of time on the horizontal axis at the mid-wall. From left to the right, each mini-plot indicates circumferential position starting at the mid-septum and wrapping to the free wall and back. The longitudinal level in the heart, from base to apex, varies from the top row to the bottom row. The multi-plot in [A] presents the evolution of circumferential strain, where more negative values indicate stronger contraction. [B] presents wall thickening [B] where more positive values indicate stronger contraction. The blue curves are pre-RT and the red curves post-RT.

### COMPUTING REGIONAL DOSE TO THE HEART

- Computation of the 3D dose field, defined on the RT planning CT images, onto the MR-based heart volume was achieved via the following steps:
- 3D masks of the lung volume were extracted independently from the planning CT and axial MR images.
- A rigid body registration was performed to align the CT-based lung masks onto the MR-based lung mask images.
- The 3D dose field, extracted as DICOM file from the treatment planning system, was subsampled to match the planning CT voxel locations.
- The 3D dose field was then aligned and subsampled to the MRI images using the previously-computed rigid-body registration results.
- For each point in the 3D material mesh, the closest voxel in the axial MRI data set was found and the estimated dose value gathered from that.
- The dose as a function of position on the heart was overlaid onto the 3D heart LV models to visualize the dose exposed to the heart (Fig. 6B).

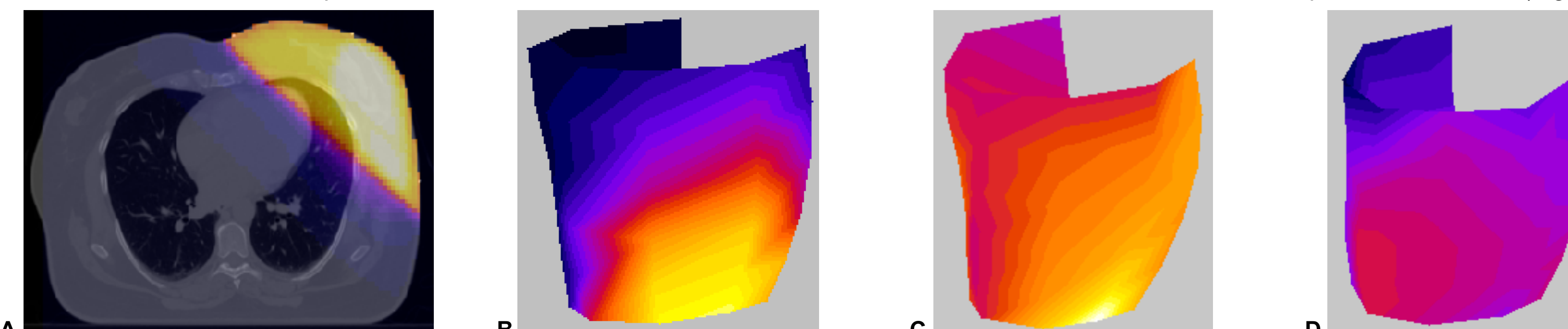


**Figure 6. Heart dose calculation :** [A] shows the RT dose on a planning CT image showing elevated exposure to the lateral LV wall and apex. [B] shows the 3D mesh of material points with an overlay of the dose distribution at each point. The yellow region indicates high exposure while black indicates low exposure (range 2 to 47 Gray). [C] and [D] shows the same material point mesh with mid-wall thickening strain at pre- and post-RT, respectively, with color scaled from 0 (black) to 1.0 (white). Thickening strain is diminished over the entire heart, with larger decrease in the regions with higher dose.

### STATISTICAL ANALYSIS

- A two-tailed paired t-test was conducted to evaluate the radiation effects to the mid-wall heart LV strains, comparing pre- versus post-RT.
- Here, a statistically significant decrease in magnitude of mean circumferential and thickening strains were found ( $p < 0.05$ ), suggesting that radiation caused lasting damage to the heart. A 95% C.I. about mean for circumferential strain change was (0.070, 0.092), with  $M=0.081$ ,  $SD=0.093$ ,  $N=288$ .

## III. CONCLUSIONS & DISCUSSION

- We have developed methods to gather and analyze pre- and post-treatment MR images, with tags, in breast cancer patients.
- The results permit regional assessment of sub-clinical changes in heart wall strain, and compare these metrics with regional radiation dose.
- Tools have been developed to visualize and quantify 3D changes in heart wall function, with correlation with radiation exposure, and perform statistical analysis of the outcomes.
- These analysis techniques are hoped to enable us to address key clinical questions:
  - Does proton therapy improve the therapeutic ratio of breast cancer radiation treatment by reducing the severity of radiation toxicity to the heart?
  - Can we identify breast cancer survivors that are at an elevated risk for cardiac disease who may benefit from proton therapy or altered RT?
  - Is there a role for cardiac imaging in routine clinical follow-up care of breast cancer patients for identification of sub-clinical cardiac toxicity?

## IV. REFERENCES

- American Cancer Society, Breast Cancer Facts and Figures 2017. (American Cancer Society, Inc., 2017).
- Overgaard M, Hansen PS, et al. Postoperative radiotherapy in high-risk premenopausal women with breast cancer who receive adjuvant chemotherapy. Danish Breast Cancer Cooperative Group 82b Trial. N Engl J Med 1997; 337: 949-55
- Darby SC, Ewertz M, et al. Risk of ischemic heart disease in women after radiotherapy for breast cancer. N Engl J Med 2013; 368: 987-98
- C.R. Correa et al. Coronary artery findings after left-sided compared with right-sided radiation treatment for early-stage breast cancer. J ClinOncol, 25 (2007), pp. 3031-3037
- O'Dell WG, Siva Kumar S. Determining prolate spheroidal modes of cardiac deformation directly from tagged heart images, 25th ISMRM Scientific Meeting and Exhibition, Honolulu, Hawaii, [6447] April 2017.
- C. C. Moore et al., "Three-dimensional systolic strain patterns in the normal human left ventricle: characterization with tagged MR imaging," Radiology 214(2), 453-466 (2000)